nature physics

SUPPLEMENTARY INFORMATION

DOI: 10.1038/NPHYS1928

Time-resolved measurement of spin-transfer-driven ferromagnetic resonance and spin torque in magnetic tunnel junctions

Chen Wang[1], Yong-Tao Cui[1], Jordan A. Katine[2], Robert A. Buhrman[1], and Daniel C. Ralph[1,3]

[1]*Cornell University, Ithaca, New York 14853, USA*

[2]*Hitachi Global Storage Technologies, San Jose Res. Ctr., San Jose, CA 95135 USA*

[3]*Kavli Institute at Cornell, Cornell University, Ithaca, NY 14853, USA*

Supplementary Note S1: Data acquisition and background subtraction in the time-domain ST-FMR measurement

In order to separate the resistance oscillation signal from the residual background oscillation of the reflected RF pulse, for any given state of the device (for magnetic field magnitude H, field direction β and bias voltage V), we identify a non-resonance reference state of the same device with equal impedance to perform background measurements. With the same impedance, the reflected signal of the same RF pulse should be the same for both states, so that the difference between the two waveforms represents the net signal produced by the resistance oscillation.

To find a reference state for the (H, β, V) state, we first determine the differential resistance R_0 of the device at the (H, β, 0) state with a low-frequency (about 1 kHz) lock-in measurement, then we increase the external magnetic field to H' (typically by 500 Oe) to shift the resonance peak completely out of the frequency range of our measurement, and finally we

DOI: 10.1038/NPHYS1928

fine-tune the field direction to β' (typically by a few degrees) so that the lock-in measurement of the resistance $R_0(H', \beta', 0)$ is equal to $R_0(H, \beta, 0)$. Throughout the measurement under the same field set (H, β) at arbitrary biases V, we use the (H', β', V) state as the reference state for the (H, β, V) state. Because the resistance is strongly dependent on bias voltage in MTJs, $R_0(H, \beta, V)$ is very different from $R_0(H, \beta, 0)$. However, if we assume that an applied bias voltage does not change the direction of the magnetization dramatically (we estimate the effect of the static spin torque can result in a change of θ by at most 3° for all our field conditions), to a good approximation $R_0(H', \beta', V) = R_0(H, \beta, V)$ should still hold because the two states have the same offset angle and bias voltage. We verified this by comparing the reflected waveform of an off-resonance RF pulse (typically with a frequency lower than the resonance of either state) at the two states, and found that the difference between the two was negligible compared to our measured signal after subtraction.

To make a time-domain measurement of the resistance oscillation at the state (H, β, V) under a given RF driving pulse, we first record the waveform at the state of interest (H, β, V) after averaging for 25 seconds (about 1250 repetitions for 2000 sampling points) (the red curve in Fig. S1a,b). We then keep the applied RF driving pulse on to maintain the same phase and amplitude, switch quickly to the reference state (H', β', V), and record the background waveform, again averaging for 25 seconds (the black curve in Fig. S1a,b). Afterwards we switch back to the original state (H, β, V) and repeat the measurement (the blue curve in Fig. S1a,b which is hardly visible since it overlaps with the red curve). It is important to record the the signal trace both before and after recording the background trace because either the falling edge of the RF pulse or the phase of the RF pulse can drift with respect to the time base of the oscilloscope by a few

picoseconds over several minutes of measurements. We discard any data taken when this drift is significant (*i.e.* more than one picosecond) during the overall measurement time of about 1.5 minutes. Finally we average the signal traces and subtract the background, giving a final result such as shown in Figures 2b and 2c in the main text. The resulting waveform is proportional to the resistance oscillation of the MTJ.

Supplementary Note S2: Comments about the effects of heating and spatially non-uniform magnetic dynamics.

We claim in the main paper that ST-FMR with time-domain detection of the resonant magnetic dynamics is much less vulnerable than competing techniques to artifacts arising from heating or nonuniform magnetic dynamics. We will expand on those issues here.

Our technique has little sensitivity to heating because, at least for a circular sample, an oscillatory temperature should not drive magnetic precession with a definite phase relationship relative to the input RF signal. Therefore, the presence of heating should not give rise to any artifact signals in a time-domain experiment in which the measurements are made following the end of the drive pulse. For a non-circular sample and an equilibrium free-layer orientation away from symmetry direction for the magnetic anisotropy, it is possible for oscillatory heating to drive precession via modulation of the magnetic anisotropy fields, but the torques we measure show reasonable agreement with the expected angular dependence ($\propto \sin\theta$) without this effect, which indicates that it is not a significant factor. Heating in our experiment might lead to a decrease in the average moment of the free layer in our samples at high bias, therefore increasing slightly the apparent value of the torkances for large $|V|$. However, we anticipate that this is a small effect unless the bias is high enough that the effective magnetic temperature approaches

DOI: 10.1038/NPHYS1928

the Curie temperature (> 800 K).

One may also question the applicability of the macrospin approximation we use to extract the value of the spin-torque vector from our measurements. Our measurements are designed to minimize the likelihood of any significant spatial nonuniformities in the magnetic dynamics, so that the macrospin model should be a good approximation. We employ small, circular samples (as small as 80 nm diameter) with an in-plane equilibrium magnetic state, take measurements in an external in-plane magnetic field of 200-400 Oe that promotes a uniform initial state, and excite only small angle precession from this state (~1° mean deflection). However, even in the presence of small deviations from the macrospin approximation, the results of ST-FMR with time-domain detection should be largely insensitive to these deviations, particularly relative to previous techniques for determining the spin torque vector. Our measurements begin with a large equilibrium offset angle between the magnetic orientation of the reference layer and the average orientation of the free layer, so that the spin torque applied throughout the free layer is large, in the same direction, and approximately uniform. By measuring resistance, we determine, to a good approximation, the average deflection induced by the spin torque over the entire free layer. Via the time-domain measurement, we also measure directly the oscillation decay rate integrated over the whole sample. Under these circumstances, average precession amplitudes we measure, and hence the values of the spin-torque vector that comprise our final result, should be determined by conservation of spin angular momentum integrated over the whole free layer (total spin angular momentum absorbed in each cycle = spin angular momentum lost to damping in each cycle), even if the magnetic dynamics may contain small spatial nonuniformities.

Supplementary Note S3: Determination of the spin transfer torque vector from the ST-FMR oscillation signal

In this derivation we assume that the dynamics of the magnetic free layer can be approximated by a simple macrospin model, and we calculate the magnetic response to an oscillating spin torque. We have commented above in Supplementary Note 2 about the possible consequences of micromagnetic effects beyond the macrospin model. Our calculation builds on the derivation of the ST-FMR signal presented in the appendix of ref. S1, with one correction and one addition. The correction is that here we take into account that the directions of the in-plane and out-of-plane components of the spin torque vector will rotate slightly relative to the sample axes as the free layer undergoes small-angle precession. The failure to take this into account in our previous paper led to a factor-of-two error in calculating the bias dependence of the effective magnetic damping, and the correction brings our results into accord with the result in references S2 and S3. The addition is that we self-consistently take into account a feedback effect,[S4] that when a DC bias is applied to a precessing magnetic tunnel junction, the resistance oscillations arising from the precession will modify the high-frequency part of the bias across the junction. This effect can become significant under conditions of large DC bias and small effective magnetic damping.

We assume that the magnetic moment of the free layer has a constant magnitude $M_s Vol$ and we denote its instantaneous direction by the unit vector $\hat{m}(t)$. We define $\hat{z}$ as the equilibrium direction of the free layer (and assume that it is within the plane of the thin-film sample to a good approximation even at non-zero bias V), $\hat{x}$ as the direction perpendicular to the film plane, and $\hat{y}$ is the in-plane direction satisfying $\hat{z} = \hat{x} \times \hat{y}$. At the equilibrium position, $\hat{m} = (0,0,1)$. Small-angle precession of the free layer in response to a DC + oscillatory voltage

DOI: 10.1038/NPHYS1928

$V(t) = V + \delta V(t) = V + \mathrm{Re}(\delta V e^{i\omega t})$ can be expressed in the form $\hat{m}(t) = (m_x(t), m_y(t), 1)$ or $\hat{m}(t) = \mathrm{Re}(m_x e^{i\omega t}, m_y e^{i\omega t}, 1)$, where $|m_x|, |m_y| << 1$. We assume that the reference magnetic layer remains fixed in the in-plane direction $\hat{M} = (0, \sin\theta, \cos\theta)$. Because of the large magnetic anisotropy of the thin film sample, $|m_x| << |m_y|$ and therefore the oscillations of the angle θ between the two magnetizations during precession can be expressed to a good approximation as $\delta\theta(t) = -\mathrm{Re}\left(m_y e^{i\omega t}\right)$.

Within the macrospin approximation, the dynamics of the free layer moment are governed by the Landau-Lifschitz-Gilbert-Slonczewski (LLGS) equation:

$$\frac{d\hat{m}}{dt} = -\gamma \hat{m} \times \vec{H}_{\mathrm{eff}} + \alpha \hat{m} \times \frac{d\hat{m}}{dt} + \gamma \frac{\tau_{\parallel}(V,\theta)}{M_s Vol} \hat{m} \times \frac{\hat{m} \times \hat{M}}{|\hat{m} \times \hat{M}|} + \gamma \frac{\tau_{\perp}(V,\theta)}{M_s Vol} \frac{\hat{m} \times \hat{M}}{|\hat{m} \times \hat{M}|}, \qquad \text{(S1)}$$

where $\tau_{\parallel}(V,\theta)$ and $\tau_{\perp}(V,\theta)$ are in-plane (Slonczewski) component and out-of-plane (field-like) components of the spin torque, written as a function of voltage and offset angle between the two layers. (Note that this equation is corrected from the form of the LLGS equation used in ref. S1 by taking into account that the in-plane and out-of-plane unit vectors will shift direction as $\hat{m}(t)$ precesses.) $\vec{H}_{\mathrm{eff}} = -N_x M_{eff} m_x \hat{x} - N_y M_{eff} m_y \hat{y}$ is the effective field acting on the free layer, with $N_x = 4\pi + H / M_{eff} \approx 4\pi$ since the in-plane field we apply (200-400 Oe) is much weaker than the easy-plane anisotropy of the film (~13 kOe). $N_y \approx H / M_{eff}$, neglecting anisotropy and interlayer coupling. $\gamma = 2\mu_B / \hbar$ is the absolute value of the gyromagnetic ratio, and α is the Gilbert damping coefficient. For small RF excitation voltages, the magnitude of the spin-torque components can be Taylor-expanded,

$$\begin{aligned}\tau_{\parallel}(V+\delta V(t),\theta+\delta\theta(t)) &= \tau_{\parallel}(V,\theta)+\frac{\partial\tau_{\parallel}}{\partial V}\delta V(t)+\frac{\partial\tau_{\parallel}}{\partial\theta}\delta\theta(t)\\ \tau_{\perp}(V+\delta V(t),\theta+\delta\theta(t)) &= \tau_{\perp}(V,\theta)+\frac{\partial\tau_{\perp}}{\partial V}\delta V(t)+\frac{\partial\tau_{\perp}}{\partial\theta}\delta\theta(t).\end{aligned} \tag{S2}$$

As noted above, the directions of the torque components also change directions slightly during precession,

$$\hat{m}\times\frac{\hat{m}\times\hat{M}}{|\hat{m}\times\hat{M}|}=-\hat{y}+m_x\cot\theta\hat{x}+m_y\hat{z},\ \frac{\hat{m}\times\hat{M}}{|\hat{m}\times\hat{M}|}=-\hat{x}-m_x\cot\theta\hat{y}+m_x\hat{z}, \tag{S3}$$

to first order in m_x and m_y. After substituting Eq. (S2) and Eq. (S3) into Eq. (S1), the time-dependent part is, to first order,

$$\begin{aligned}\frac{dm_x(t)}{dt} &= -\gamma m_y(t)N_yM_{eff}-\alpha\frac{dm_y(t)}{dt}+\frac{\gamma}{M_SVol}\tau_{\parallel}m_x(t)\cot\theta-\frac{\gamma}{M_SVol}\left[\frac{\partial\tau_{\perp}}{\partial V}\delta V(t)-\frac{\partial\tau_{\perp}}{\partial\theta}m_y(t)\right],\\ \frac{dm_y(t)}{dt} &= \gamma m_x(t)N_xM_{eff}+\alpha\frac{dm_x(t)}{dt}-\frac{\gamma}{M_SVol}\left[\frac{\partial\tau_{\parallel}}{\partial V}\delta V(t)-\frac{\partial\tau_{\parallel}}{\partial\theta}m_y(t)\right]-\frac{\gamma}{M_SVol}\tau_{\perp}m_x(t)\cot\theta.\end{aligned} \tag{S4}$$

Using the notation $m_x(t)=\mathrm{Re}(m_xe^{i\omega t})$, $m_y(t)=\mathrm{Re}(m_ye^{i\omega t})$ and $\delta V(t)=\mathrm{Re}(\delta Ve^{i\omega t})$,

$$\begin{aligned}i\omega m_x &= -m_y\left(\gamma N_yM_{eff}+i\alpha\omega\right)+\frac{\gamma}{M_SVol}\tau_{\parallel}m_x\cot\theta-\frac{\gamma}{M_SVol}\left[\left.\frac{\partial\tau_{\perp}}{\partial V}\right|_{\theta}\delta V-\left.\frac{\partial\tau_{\perp}}{\partial\theta}\right|_{V}m_y\right]\\ i\omega m_y &= m_x\left(\gamma N_xM_{eff}+i\alpha\omega\right)-\frac{\gamma}{M_SVol}\left(\left.\frac{\partial\tau_{\parallel}}{\partial V}\right|_{\theta}\delta V-\left.\frac{\partial\tau_{\parallel}}{\partial\theta}\right|_{V}m_y\right)-\frac{\gamma}{M_SVol}\tau_{\perp}m_x\cot\theta.\end{aligned} \tag{S5}$$

In our experiments, we apply an external RF voltage $V_{in}(t)=V_{in}\,\mathrm{Re}(e^{i\omega t})$ to the sample, which is related to the true voltage and current at the sample by the following microwave circuit equations,

$$\begin{aligned}V(t) &= V+\mathrm{Re}(\delta Ve^{i\omega t})=V+V_{in}\,\mathrm{Re}(e^{i\omega t})+\mathrm{Re}(V_{ref}e^{i\omega t})\\ I(t) &= I+\mathrm{Re}(\delta Ie^{i\omega t})=I+V_{in}\,\mathrm{Re}(e^{i\omega t})/(50\ \Omega)-\mathrm{Re}(V_{ref}e^{i\omega t})/(50\ \Omega)\end{aligned} \tag{S6}$$

Also, the resistance of the MTJ imposes the restrictions,

$$V(t)=V+\left.\frac{\partial V}{\partial I}\right|_{\theta}\delta I(t)+\left.\frac{\partial V}{\partial\theta}\right|_{I}\delta\theta(t)=V+R_0\delta I(t)+I\left.\frac{\partial R}{\partial\theta}\right|_{I}\delta\theta(t) \tag{S7}$$

DOI: 10.1038/NPHYS1928

where $R_0 = \partial V / \partial I|_\theta$ is the differential resistance of the MTJ, and $R = V / I$ is the DC resistance of the MTJ. From Eq. (S6) and Eq. (S7), together with the relation $\delta\theta(t) = \mathrm{Re}(-m_y e^{i\omega t})$,

$$V_{in} + V_{ref} = R_0 \frac{V_{in} - V_{ref}}{(50\ \Omega)} - I \frac{\partial R}{\partial \theta}\bigg|_I m_y . \tag{S8}$$

Therefore,

$$V_{ref} = \frac{R_0 - (50\ \Omega)}{R_0 + (50\ \Omega)} V_{in} - \frac{(50\ \Omega)}{R_0 + (50\ \Omega)} I \frac{\partial R}{\partial \theta}\bigg|_I m_y \tag{S9}$$

and

$$\delta V = V_{in} + V_{ref} = \frac{2R_0}{R_0 + (50\ \Omega)} V_{in} - \frac{(50\ \Omega)}{R_0 + (50\ \Omega)} I \frac{\partial R}{\partial \theta}\bigg|_I m_y . \tag{S10}$$

By expressing the magnetic equations of motion in terms of the applied RF drive V_{in} (which does not change due to feedback when the free layer rotates) rather than the actual oscillating voltage across the tunnel junction δV (which does change due to feedback), we can account for the feedback self consistently. Therefore we substitute Eq. (S10) into Eq. (S5):

$$\begin{aligned} i\omega m_x &= -m_y \left(\gamma N_y M_{eff} + i\alpha\omega\right) \\ &\quad - \frac{\gamma}{M_S Vol}\left[\frac{2R_0}{R_0 + (50\ \Omega)} \frac{\partial \tau_\perp}{\partial V}\bigg|_\theta V_{in} - \left(\frac{\partial \tau_\perp}{\partial \theta}\bigg|_V + \frac{(50\ \Omega)}{R_0 + (50\ \Omega)} I \frac{\partial R}{\partial \theta}\bigg|_I \frac{\partial \tau_\perp}{\partial V}\bigg|_\theta\right) m_y - \tau_\parallel^0 m_x \cot\theta\right] \\ i\omega m_y &= m_x \left(\gamma N_x M_{eff} + i\alpha\omega\right) \\ &\quad - \frac{\gamma}{M_S Vol}\left[\frac{2R_0}{R_0 + (50\ \Omega)} \frac{\partial \tau_\parallel}{\partial V}\bigg|_\theta V_{in} - \left(\frac{\partial \tau_\parallel}{\partial \theta}\bigg|_V + \frac{(50\ \Omega)}{R_0 + (50\ \Omega)} I \frac{\partial R}{\partial \theta}\bigg|_I \frac{\partial \tau_\parallel}{\partial V}\bigg|_\theta\right) m_y + \tau_\perp^0 m_x \cot\theta\right] \end{aligned} \tag{S11}$$

Solving Eq. (S11) for m_y yields

$$m_y = \frac{R_0}{R_0 + (50\ \Omega)} \frac{\gamma V_{in}}{M_S Vol} \frac{2\omega}{\left(\omega^2 - \omega_m^2 - i2\omega\Gamma_0\right)}\left[i \frac{\partial \tau_\parallel}{\partial V}\bigg|_\theta + \frac{\gamma N_x M_{eff}}{\omega} \frac{\partial \tau_\perp}{\partial V}\bigg|_\theta\right], \tag{S12}$$

which close to resonance $\omega \approx \omega_m$ becomes

$$m_y = \frac{R_0}{R_0 + (50\ \Omega)} \frac{\gamma V_{in}}{M_S Vol} \frac{1}{\omega - \omega_m - i\Gamma_0} \left[i \frac{\partial \tau_{\parallel}}{\partial V}\bigg|_{\theta} + \frac{\gamma N_x M_{eff}}{\omega_m} \frac{\partial \tau_{\perp}}{\partial V}\bigg|_{\theta} \right], \tag{S13}$$

where

$$\omega_m \approx \gamma M_{eff} \sqrt{N_x \left[N_y - \frac{1}{M_{eff} M_S Vol} \left(\frac{\partial \tau_{\perp}}{\partial \theta}\bigg|_{V} + \frac{(50\ \Omega)}{R_0 + (50\ \Omega)} I \frac{\partial R}{\partial \theta}\bigg|_{I} \frac{\partial \tau_{\perp}}{\partial V}\bigg|_{\theta} \right) \right]} \tag{S14}$$

$$\Gamma_0 \approx \frac{\alpha \gamma M_{eff} (N_x + N_y)}{2} - \frac{\gamma}{2 M_s Vol} \left(\tau_{\parallel} \cot\theta + \frac{\partial \tau_{\parallel}}{\partial \theta}\bigg|_{V} + \frac{(50\ \Omega)}{R_0 + (50\ \Omega)} I \frac{\partial R}{\partial \theta}\bigg|_{I} \frac{\partial \tau_{\parallel}}{\partial V}\bigg|_{\theta} \right). \tag{S15}$$

Substituting Eq. (S13) in Eq. (S9), we have for the reflected signal

$$\begin{aligned} V_{ref} = & \frac{R_0 - (50\ \Omega)}{R_0 + (50\ \Omega)} V_{in} \\ & - \frac{(50\ \Omega)}{R_0 + (50\ \Omega)} \left(\frac{R_0}{R_0 + (50\ \Omega)} \right) I \frac{\partial R}{\partial \theta}\bigg|_{I} \frac{\gamma}{M_S Vol} \frac{1}{(\omega - \omega_m - i\Gamma_0)} \left[i \frac{\partial \tau_{\parallel}}{\partial V}\bigg|_{\theta} + \frac{\gamma N_x M_{eff}}{\omega_m} \frac{\partial \tau_{\perp}}{\partial V}\bigg|_{\theta} \right] V_{in}, \end{aligned} \tag{S16}$$

where the first term is the measured background V_{bg} in our experiment, and the second term is the measured signal arising from the resistance oscillation V_{sig}. Therefore the normalized complex precession amplitude $Ae^{i\Phi}$ that we analyze in our time-domain experiment takes the form

$$Ae^{i\Phi} = V_{sig} / V_{bg} = - \frac{R_0 (50\ \Omega)}{[R_0 - (50\ \Omega)][R_0 + (50\ \Omega)]} I \frac{\partial R}{\partial \theta}\bigg|_{I} \frac{\gamma}{M_S Vol} \frac{1}{(\omega - \omega_m - i\Gamma_0)} \left[i \frac{\partial \tau_{\parallel}}{\partial V}\bigg|_{\theta} + \frac{\gamma N_x M_{eff}}{\omega_m} \frac{\partial \tau_{\perp}}{\partial V}\bigg|_{\theta} \right]. \tag{S17}$$

This is a convenient quantity for analysis because amplifier gains and transmission losses cancel on account of the normalization. At the resonance frequency,

$$A_{n,\max} e^{i\Phi_m} = \frac{R_0 (50\ \Omega)}{[R_0 - (50\ \Omega)][R_0 + (50\ \Omega)]} I \frac{\partial R}{\partial \theta}\bigg|_{I} \frac{\gamma}{M_S Vol\ \Gamma_0} \left[\frac{\partial \tau_{\parallel}}{\partial V}\bigg|_{\theta} - i \frac{\gamma N_x M_{eff}}{\omega_m} \frac{\partial \tau_{\perp}}{\partial V}\bigg|_{\theta} \right]. \tag{S18}$$

From this, and using that $\gamma = 2\mu_B / \hbar$, we have the final expression we use to evaluate the time-

DOI: 10.1038/NPHYS1928

domain results [Equations (2) and (3) in the paper].

$$\left.\frac{\partial\tau_{\parallel}}{\partial V}\right|_{\theta} = \cos\Phi_m \frac{[R_0-(50\Omega)][(R_0+50\Omega)]}{R_0(50\Omega)}\frac{\hbar}{2}\frac{M_S Vol}{\mu_B I}\left(\left.\frac{\partial R}{\partial\theta}\right|_I\right)^{-1}\Gamma_0 A_{m,\max}, \tag{S19}$$

$$\left.\frac{\partial\tau_{\perp}}{\partial V}\right|_{\theta} = -\sin\Phi_m \frac{[R_0-(50\Omega)][(R_0+50\Omega)]}{R_0(50\Omega)}\frac{\hbar}{2}\frac{M_S Vol}{\mu_B I}\left(\left.\frac{\partial R}{\partial\theta}\right|_I\right)^{-1}\frac{\Gamma_0 A_{m,\max}}{\Omega_{\perp}}. \tag{S20}$$

Here $\Omega_{\perp}\approx 4\pi M_{eff}\gamma/\omega_m$. We have only to verify that the quantity Γ_0 introduced above as the half width at half maximum of the FMR lineshape has the same value as the decay rate Γ of the damped resistance oscillations in the time-domain experiment.

To prove this, we analyze the equation of motion in the case that $V_{in}(t)=0$, in the presence of a DC current. Noting that $\delta V(t)=\frac{(50\ \Omega)}{R_0+(50\ \Omega)} I\left.\frac{\partial R}{\partial\theta}\right|_I m_y(t)$ from Eq. (S10) and substituting $m_x(t)=\mathrm{Re}(m_x e^{(-\Gamma+i\omega)t})$, $m_y(t)=\mathrm{Re}(m_y e^{(-\Gamma+i\omega)t})$ and $\delta V(t)=\mathrm{Re}(\delta V e^{(-\Gamma+i\omega)t})$ into Eq. (S4), we have

$$\begin{aligned}(-\Gamma+i\omega)m_x &= -m_y\left(\gamma N_y M_{eff}+i\alpha\omega-\alpha\Gamma\right)\\ &\quad+\frac{\gamma}{M_S Vol}\tau_{\parallel}m_x\cot\theta-\frac{\gamma}{M_S Vol}\left[\left.\frac{\partial\tau_{\perp}}{\partial V}\right|_{\theta}\frac{(50\Omega)}{R_0+(50\Omega)}I\left.\frac{\partial R}{\partial\theta}\right|_I-\left.\frac{\partial\tau_{\perp}}{\partial\theta}\right|_V\right]m_y\\ (-\Gamma+i\omega)m_y &= m_x\left(\gamma N_x M_{eff}+i\alpha\omega-\alpha\Gamma\right)\\ &\quad-\frac{\gamma}{M_S Vol}\left(\left.\frac{\partial\tau_{\parallel}}{\partial V}\right|_{\theta}\frac{(50\Omega)}{R_0+(50\Omega)}I\left.\frac{\partial R}{\partial\theta}\right|_I-\left.\frac{\partial\tau_{\parallel}}{\partial\theta}\right|_V\right)m_y-\frac{\gamma}{M_S Vol}\tau_{\perp}m_x\cot\theta.\end{aligned} \tag{S21}$$

These equations determine the natural frequency ω and the decay rate Γ of the damped resistance oscillation,

$$\omega\approx\gamma M_{eff}\sqrt{N_x\left[N_y-\frac{1}{M_{eff}M_S Vol}\left(\left.\frac{\partial\tau_{\perp}}{\partial\theta}\right|_V+\frac{(50\ \Omega)}{R_0+(50\ \Omega)}I\left.\frac{\partial R}{\partial\theta}\right|_I\left.\frac{\partial\tau_{\perp}}{\partial V}\right|_{\theta}\right)\right]} \tag{S22}$$

$$\Gamma\approx\frac{\alpha\gamma M_{eff}(N_x+N_y)}{2}-\frac{\gamma}{2M_s Vol}\left(\tau_{\parallel}\cot\theta+\left.\frac{\partial\tau_{\parallel}}{\partial\theta}\right|_V+\frac{(50\ \Omega)}{R_0+(50\ \Omega)}I\left.\frac{\partial R}{\partial\theta}\right|_I\left.\frac{\partial\tau_{\parallel}}{\partial V}\right|_{\theta}\right). \tag{S23}$$

The frequency ω in Eq. (S22) is identical to the resonance frequency of ST-FMR in Eq. (S14), and the decay rate Γ is indeed equal to Γ_0, the half linewidth of the ST-FMR resonance.

If we make further approximations in Eq. (S23) that $\left.\frac{\partial \tau_{\parallel}}{\partial \theta}\right|_V >> \frac{(50\ \Omega)}{R_0 + (50\ \Omega)} I \left.\frac{\partial R}{\partial \theta}\right|_I \left.\frac{\partial \tau_{\parallel}}{\partial V}\right|_\theta$ and use that for a tunnel junction $\tau_{\parallel} \propto \sin\theta$ (so that $\tau_{\parallel} \cot\theta = \partial \tau_{\parallel} / \partial \theta|_V$),[5] we have

$$\Gamma = \Gamma_0 \approx \frac{\alpha \gamma M_{eff}(N_x + N_y)}{2} - \frac{\gamma}{M_s Vol} \left.\frac{\partial \tau_{\parallel}}{\partial \theta}\right|_V . \qquad \text{(S24)}$$

The second term on the right differs by a factor of 2 from Eq. (A9) in ref. S1, on account of the correction we have made in the form of the LLGS equation [Eq. (S1) above], and it brings our result into accord with the calculations of Petit et al.[S2,S3] This correction also improves the agreement between theory and experiment for the measurements for the bias dependence of the effective magnetic damping α_{eff} (defined as $\Gamma_0 = \alpha_{eff} \gamma M_{eff}(N_x + N_y)/2$), plotted in Fig. 7(a) of ref. S1. The correction does not affect the analysis of any of our other previous results to within experimental accuracy.

Supplementary Note S4: Quantitative analysis of the decay rate of the resistance oscillations

By our analysis in Supplementary Note S3 above, the decay rate Γ measured from the time-domain resistance oscillations and the resonance half linewidth Γ_0 measured using DC-detected ST-FMR should be equal and can be expressed in terms of the effective damping α_{eff} of the free layer as $\Gamma = \Gamma_0 = \alpha_{eff} \gamma M_{eff}(N_x + N_y)/2$. Using $N_x \approx 4\pi$, $N_y \approx 0$, and $4\pi M_{eff} = 13 \pm 1$ kOe, we plot in Fig. S2 the bias dependence of the effective damping we determine from both Γ

DOI: 10.1038/NPHYS1928

(using the time-resolved measurements) and Γ_0 (using DC-detected ST-FMR). We observe quantitative agreement between the two methods within our experimental uncertainties. From this we conclude that the time-domain decay rate corresponds to the true decay of amplitude for the magnetization dynamics, with negligible contribution from dephasing between repetitions of the measurement. In the presence of significant dephasing between experimental repetitions, the time-domain oscillations would decay more quickly than the damping rate indicated by the ST-FMR linewidth.

From Eq. (S23), and taking into account that $\tau_{\parallel} \propto \sin\theta$, the effective damping should be related to the Gilbert damping and the spin transfer torque as:

$$\alpha_{eff} \approx \alpha - \frac{1}{M_s Vol M_{eff}(N_x + N_y)}\left(\left.\frac{\partial \tau_{\parallel}}{\partial \theta}\right|_V + \frac{(50\ \Omega)}{R_0 + (50\ \Omega)} I \left.\frac{\partial R}{\partial \theta}\right|_I \left.\frac{\partial \tau_{\parallel}}{\partial V}\right|_\theta \right) \qquad \text{(S25)}$$

The Gilbert damping coefficient α for the samples can be determined from the data in Fig. S2 near zero bias. We find α = 0.016 ± 0.001 for sample 2 (shown in Fig. S2) and α = 0.014 ± 0.001 for sample 1 (not shown). These values are at the high end of the typical reported value of Gilbert damping of CoFeB films,[S6] possibly due to sidewall oxidation[S7] or coupling to the SAF pinned layer. Using our measured spin torque and torkance results (Fig. 3 of the main paper), we can check whether the bias dependence of the damping that we measure is consistent with the prediction in Eq. (S25) (dashed lines in Fig. S2). We find good agreement, to within the level of uncertainty of the damping measurements. We should also note that the bias dependence of the effective damping could also be affected by factors such as heating and/or changes in the degree of spatial uniformity for the magnetic precession that are not included in our model.

Supplementary Note S5: Calibration of the resistance of the MTJ and the applied bias voltage at high biases

Calculation of the spin transfer torque based on Equations (2) and (3) of the main paper requires accurate measurements of the resistance of the MTJ (which depends on the applied magnetic field and bias voltage) and also the voltage provided by the square pulse during the time-domain ST-FMR measurement. Here we describe our calibration procedures for determining these quantities.

At low biases, the bias dependence of the differential resistance of the MTJ can be measured by a conventional low-frequency lock-in amplifier technique. However, this method is not practical at very high bias, because applying a large constant bias can damage or destroy the tunnel barrier even if the bias is still comfortably below the breakdown voltage for nanosecond pulses. In order to calibrate the resistance of the MTJ at high biases accurately, we utilize the fact that the amplitude of a reflected RF pulse from the MTJ depends on the differential resistance. For an incident RF pulse $V(t) = V_{in}\,\mathrm{Re}(e^{i\omega t})$ with small amplitude V_{in} having a frequency far away from resonance (so that it does not excite magnetic dynamics), the reflected amplitude is simply (from Eq. (S16))

$$V_{ref} = \frac{R_0 - (50\ \Omega)}{R_0 + (50\ \Omega)} V_{in}, \tag{S26}$$

where R_0 is the differential resistance, dependent on the offset angle and bias voltage across the MTJ. For calibration, we measure the reflected amplitude V_{ref} using the same incident RF pulse for the whole range of different resistances we can access safely with a DC bias, ranging from a maximum value corresponding to the anti-parallel state with V = 0 to a minimum value corresponding to the parallel state with V = 0.35 V in our case. At the same time, we measure the differential resistances for all these states using a lock-in amplifier. This procedure provides the

DOI: 10.1038/NPHYS1928

basis to convert V_{ref} to R_0. We then apply square-wave pulses of various amplitudes (which can access higher biases) instead of a true DC voltage, and sweep the directions of the magnetic field (which changes the offset angle between the two moments), while measuring the reflected amplitude V_{ref} of the RF pulse. Using this process, we map out R_0 as a function of offset angle and nominal amplitude V_{sq} of the applied square pulse (read from the set output voltage of the pulse generator), *i.e.* $R_0 = R_0(\theta, V_{sq})$.

It should be noted that the calibration described so far has determined the differential resistance R_0 for any given square pulse (with nominal pulse amplitude V_{sq}), but the true value of bias voltage V across the MTJ is not yet known. The equivalent bias V under a square pulse depends on the DC resistance R:

$$V = \frac{2R}{R + (50\ \Omega)} \lambda V_{sq}, \tag{S27}$$

where λ is a constant ratio between the nominal pulse amplitude and the true incoming pulse amplitude arriving on the device, determined by transmission and contact losses. In order to calibrate V for any given V_{sq}, we must first determine the coefficient λ. Taking advantage of the significant bias dependence of resistance of the MTJ (especially in the anti-parallel state), this can be done easily within the DC-accessible range $|V| < 0.35$ V where both R and R_0 can be directly measured by low-frequency techniques. We compare the value of R_0 as a function of V_{sq} we measure from the microwave reflection method and a separate measurement of R_0 as a function of V by low-frequency lock-in technique. This comparison provides a quantitative measurement of the bias V on the MTJ for any V_{sq} up to $|V| = 0.35$ V, which is sufficient to determine λ using Eq. (S27). We have also further tested that Eq. (S27) with this calibrated λ is indeed still accurate for higher bias (larger pulse height) by applying a large square pulse

together with a DC voltage in the opposite polarity so that the added bias voltage is within the DC-accessible range and therefore can be calibrated.

After we determine λ, we must still determine the DC resistance R in order to use Eq. (S27) to determine the true bias voltage V at high bias. Since we have measured differential resistance $R_0 = R_0(\theta, V_{sq})$ using the RF pulse reflection method as discussed above, V, I and R can all be determined by numerical integration from low bias to higher bias. Because $R=V/I$, we can write Eq. (S27) as $2\lambda V_{sq} = V + I(50\ \Omega)$, which can then be used to determine the relationship between an incremental change in incident pulse height and the incremental change in voltage or current that it produces:

$$dV = 2\lambda dV_{sq} \Big/ \left[1 + \frac{(50\ \Omega)}{R_0}\right] \quad \text{or} \quad dI = 2\lambda dV_{sq} \Big/ \left[R_0 + (50\ \Omega)\right], \tag{S28}$$

where $R_0 = dV/dI$ is the differential resistance. Therefore,

$$\begin{aligned} V(\theta,V_{sq}) &= \int_0^{V_{sq}} \frac{2\lambda R_0(\theta,V_{sq})}{R_0(\theta,V_{sq}) + (50\ \Omega)} dV_{sq} \\ I(\theta,V_{sq}) &= \int_0^{V_{sq}} \frac{2\lambda}{R_0(\theta,V_{sq}) + (50\ \Omega)} dV_{sq} \\ R(\theta,V_{sq}) &= \frac{V(\theta,V_{sq})}{I(\theta,V_{sq})} \end{aligned} \tag{S29}$$

We can thus obtain calibrated values of V, R and R_0 at any given θ and V_{sq}, as required to calculate the spin-transfer torque using Equations (2) and (3) of the main paper.

DOI: 10.1038/NPHYS1928

References:

S1. Wang, C., Cui, Y.-T., Sun, J. Z., Katine, J. A., Buhrman, R. A. & Ralph, D. C. Bias and angular dependence of spin-transfer torque in magnetic tunnel junctions. *Phys. Rev. B* **79**, 224416 (2009).

S2. Petit, S. *et al.* Spin-torque influence on the high-frequency magnetization fluctuations in magnetic tunnel junctions. *Phys. Rev. Lett.* **98,** 077203 (2007).

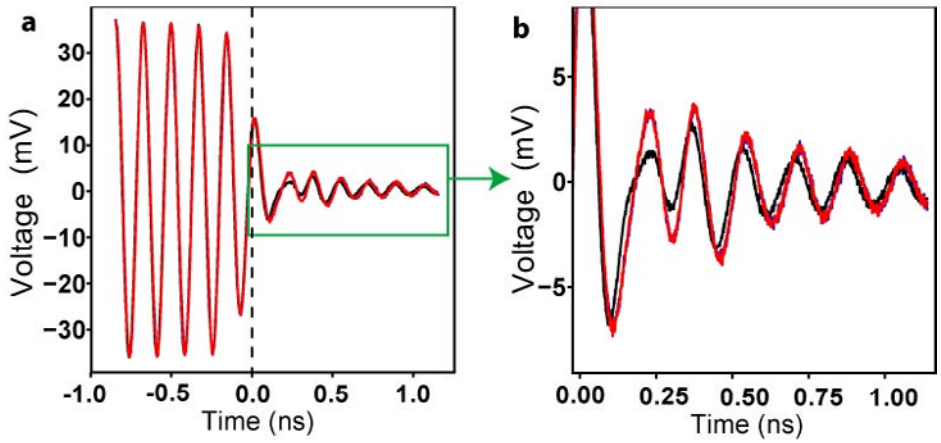
S3. Petit, S. *et al.* Influence of spin-transfer torque on thermally activated ferromagnetic resonance excitations in magnetic tunnel junctions. *Phys. Rev. B* **78,** 184420 (2008).

S4. Garzon, S., Webb, R. A., Covington, M., Kaka, S. & Crawford, T. M. Effect of resistance feedback on spin torque-induced switching of nanomagnets. J. Magn. Magn. Mater. **321,** 3225 (2009).

S5. Slonczewski, J. C. Currents, torques, and polarization factors in magnetic tunnel junctions. *Phys. Rev. B* **71,** 024411 (2005).

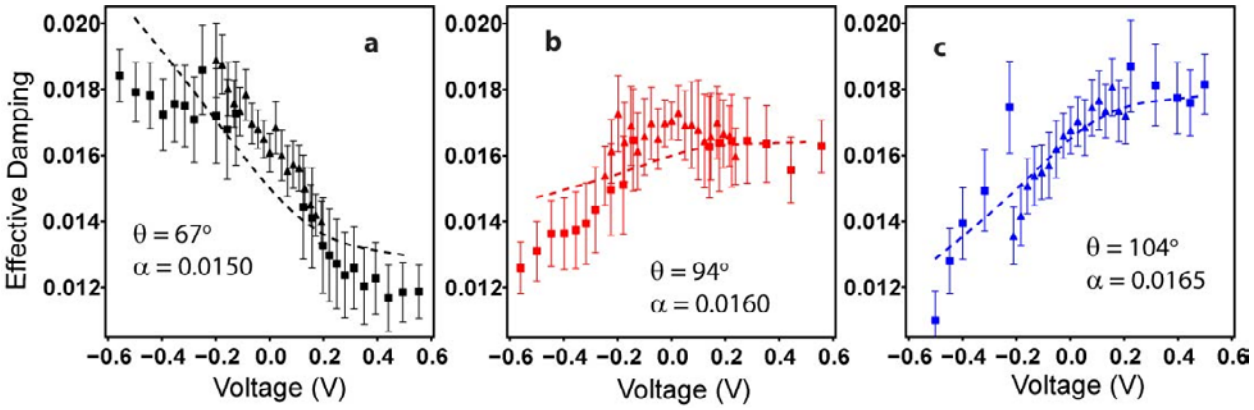
S6. Fuchs, G. D. *et al.* Spin-torque ferromagnetic resonance measurements of damping in nanomagnets. *Appl. Phys. Lett.* **91,** 062507 (2007).

S7. Ozatay, O. *et al.* Sidewall oxide effects on spin-torque- and magnetic-field-induced reversal characteristics of thin-film nanomagnets. *Nature Mater.* **7,** 567 (2008).



Supplementary Figure S1: Background subtraction. a, The raw signal and background waveform traces used to measure the resistance oscillation signal in Fig. 2 of the main paper. The red curve and the blue curve (overlapping with the red curve and hardly visible) are the reflected voltage waveforms measured by the sampling oscilloscope for a 5.8 GHz RF driving pulse, taken from sample 1 under the following bias parameters: magnetic field H = 200 Oe, field direction β = 90°, offset angle θ = 85°, V = 0.38 V. The black curve is the reflected voltage waveform measured for the same driving pulse but for a different magnetic field H = 600 Oe, β = 94°, so as to provide a non-resonant background measurement. **b**, Zoom-in of the curves within the green box in **a**. Subtraction of the background curve from the measured waveform near resonance yields the result in Fig. 2b and 2c of the main paper.

DOI: 10.1038/NPHYS1928



Supplementary Figure S2: Measurement of effective damping. (squares) Bias dependence of the effective damping α_{eff} determined from the decay rate Γ of the resistance oscillation in the time-resolved measurements (averaging over RF driving frequencies close to the resonance peak). (triangles) Bias dependence of the effective damping determined from the linewidth Γ_0 of the resonance peak in DC-detected ST-FMR measurements. The different panels correspond to different initial offset angles θ for the same sample (sample 2). The dashed lines show the effective damping predicted by Eq. (S25), using the in-plane torkances measured in the time-resolved experiment. Slightly different values of the Gilbert damping α were used for different offset angles to provide better fits of the data.